Computer Aided Diagnosis Of MR Images

Snehal G. Shewale
Computer Department
L.G.N.S.C.O.E
Nashik, India

Anuja A. Kumbharde
Computer Department
L.G.N.S.C.O.E
Nashik, India

Chetan H. Patil
Computer Department
L.G.N.S.C.O.E
Nashik, India

Bharat G. Gore
Computer Department
L.G.N.S.C.O.E
Nashik, India

_____

Abstract: **Background: Spine magnetic resonance image (MRI) plays a very important role in the diagnosis of various spinal diseases, such as disc degeneration, scoliosis, and osteoporosis. Accurate localization and segmentation of the intervertebral disc (IVD) in spine MRI can help accelerate the diagnosis time and assist in the treatment by providing quantitative parameters. In this paper, a method based on Gabor filter bank is proposed for IVD localization and segmentation.**
In this,the structural features of IVDs are extracted using a Gabor filter bank. Second, the Gabor features of spine are calculated and spinal curves are detected. Third, the Gabor feature images (GFI) of IVDs are calculated and adjusted according to the spinal curves. Fourth, the IVDs are localized by clustering analysis with GFI. Finally, an optimum grayscale-based algorithm with self-adaptive threshold, combined with the localization results and Gabor features of the spine, is performed for IVDs segmentation.

Keywords: Magnetic resonance image, intervertebral disc, Localization.
_____

I.   INTRODUCTION

Spinal diseases, such as low-back pain (LBP), are common diseases and are harmful to human health. LBP is a common symptom with considerable social and economic repercussions. LBP is experienced by 25 to 50 % of the adult population in the United States. The healthcare costs for spine pain (mainly for LBP) is increasing every year in the United States. The degeneration of intervertebral discs (IVDs) is the main factor resulting in chronic LBP and disability . Analysis of magnetic resonance imaging (MRI), including disc localization and segmentation, is the Procedure for Paper Submission degenerative disk disease and evaluate the spinal cord, ligaments, and lesions, as it provides high-resolution, high-contrast images in serial contiguous slices. Previously, disc localization and segmentation in spine MRI was performed by the radiologists manually, and the results depended on the a priori knowledge and experience. Additionally, manual localization and segmentation is laborious and lacks reproducibility between observers.

Therefore, it is necessary to develop methods to localize and segment the IVDs automatically. An accurate localization and segmentation with computer-aided diagnosis (CAD) for discs in spine MRI would be useful in the quantification of disc degeneration, diagnosis of the disease, and computer-assisted spine surgery . But, the differences in size, shape, appearance, intensity of different IVDs, and the ambiguous IVD boundaries and similar intensity with surrounding tissues may increase the difficulty of recognition. Model-based methods are often used to analyze IVDs in past years. Alomari proposed a two-level probabilistic model for localization of discs from MRI. Michopoulou also presented a semiautomatic approach to segment both normal and degenerated lumbar IVDs. Peng used a model-based searching method to localize whole spine discs. Castro segmented the IVDs using active contour models and fuzzy C-means. Haq proposed a segmentation approach based on the discrete simplex surface model. Law employed a novel anisotropic-oriented flux model to segment the IVDs. These methods are effective for IVDs with CAD, but need manual operations or user-controlled manners to refine the results.

However, they only detect six discs with their graphical model and require the existence of both T1 and T2 scans to detect the spinal cord. Ghosh achieved the localization of lumbar discs using histogram of oriented gradients

along with SVM. Furthermore, a method is proposed to segment all the tissues simultaneously in a lumbar sagittal MRI, using an auto-context approach, instead of any explicit shape features or models.
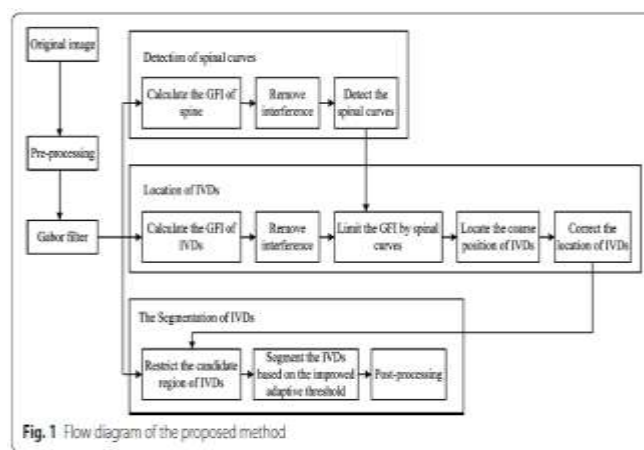
It made strong use of heuristics and information from complementary axial scans. Cheng used a machine-learning based technique to localize and segment the 3D IVDs from MRIs. The IVD localization was done by estimating the image displacements from a set of randomly sampled 3D image patches to the IVD center. The IVDs were segmented by classifying image pixels around disc centers as background or foreground. Kelm combined marginal space learning with a generative anatomical network to detect and label the IVDs. An optional case-adaptive segmentation approach was proposed to segment the IVDs and vertebrae in MRI and CT, respectively. The presence of intensity in homogeneities may influence the quality of intensity-based feature extraction.

Extraction of information and its service for localization and segmentation of IVDs is important. Compared with other tissues in spinal MRI, IVD has the Zhu et al. BioMed Eng OnLine (2016) 15:32 Page 3 of 15 distinctly characteristic, relatively regular and similar elliptic structure. The extraction of IVD structure information, such as shape and direction, and avoiding interference from peripheral tissues is challenging. The Gabor filter, a windowed Fourier transform, derives from the work of Gabor D. Daugman extended the Gabor filter to two-dimensional (2D) spatial position. Given the biological background and the optimal space and spatial-frequency localization of Gabor filter it is widely used for image process applications. When the direction and frequency of the objects in an image are consistent with those of 2D-Gabor filters, the wavelet transformation has a strong response.

Since the IVDs in spinal MRI are regular and ellipse-shaped, the recognition of IVDs is possible by transformation of Gabor filtering. We propose an unsupervised computer-aided IVD localization and segmentation method based on Gabor filter bank, which does not require any training. Among various wavelet bases, the 2D Gabor filters provide good resolution both in temporal and frequency domains, and provide the optimal basis to extract local features because of: (1) Frequency motivation: both multi-resolution and multi-orientation properties of Gabor wavelet are optimal for measuring local spatial frequencies (2) morphology motivation: it distorts the tolerance space for pattern recognition tasks. The proposed method adopts Gabor filters to extract the structural features of IVDs, and localize and segment the IVDs. The information from the Gabor filter is capable of increasing the accuracy and automation degree for IVD localization and segmentation.

II. METHODOLOGY USED

Flow diagram: The flow chart of the proposed method is shown in Fig. 1. It includes the Gabor filter design, detection of spinal curves, localization of IVDs, and segmentation of IVDs. First, a set of 2D-Gabor filters, with different frequencies and directions, are used in image filtering to get a series of Gabor images. Second, Gabor features of the spine are calculated and the spinal curves are detected. Third, the Gabor features images (GFI) of IVDs are calculated and limited by spinal curves. Fourth, the IVD localization is performed by cluster analysis. Correction of localization is done to improve the accuracy of localization results. Last, segmentation of IVDs is performed based on the Gabor filter, localization results, and an improved self-adaptive threshold.

Fig. 1 Flow diagram of the proposed method

A. Setting of the Gabor filter:

Effective extraction of the IVD features depends on the setting of the Gabor kernel function. Due to the elliptic shape of IVDs, the parameter _ of Gabor kernel is different in horizontal x and vertical y direction. In addition, there is an angle between the IVDs and the horizontal plane. Therefore, the Gabor kernel is defined as : where, x′ = x cos _μ + y sin _μ, y′ = −x sin _μ + y cos _μ represent the spatial locations of pixels. In spatial domain, the parameters _μ, __, and _ represent the direction, wavelength, and Gaussian window of Gabor filter bank, respectively.

International Journal of Science Technology Management and Research
Volume 1 , Issue 8 , November 2016
www.ijstmr.com

The parameters of Gabor are set as follows: to describe the local features of images, a Gabor filter bank has S directions and K scales (usually S = 8, K = 5) . However, the IVDs have a relatively uniform size and the differences among their angles are smaller. A Gabor filter bank in 16 directions with five scales is used. The upper frequency limit _max = _ 2 is set according to the experience. Since the size of IVDs is relatively uniform, the frequency spacing factor f = √4 2 is set to obtain the effective center frequency. The effective radius of the Gaussian window is expressed as rv = 2√2_ _v . According to the characteristics of the IVD (the width occupies at least 25 pixels and the thickness is about half of the width), _x = 3k _v , _y = 6k _v (where k = √2 ln 2). The symmetric Gabor kernel window with the size of 31 × 31 is used, based on experiment.

B. Localization Of Ivds-:

- **Detection of spinal curves**

In order to reduce the impact of background on localization and segmentation, the spinal edges are detected to narrow the searching range. Since the spinal curves are nearly vertical, the spinal GFI is obtained by subtracting the GFI of horizontal direction from that of vertical direction. Taking Gv,μ as the Gabor-filtered image with direction μ and

Gabor filter bank is Real components of Gabor filter bank in S directions with K scales (S = 16, K = 5) scale v, the spinal GFI Gspine can be described as Eq. : where v ∈ C = {0, 1, . . . , S − 1}, μ ∈ U = {0, 1, . . . , K − 1}, U1 = {0, 1, 2, 3, 4, 5, 14, 15} , and U2 = {7, 8, 9, 10, 11} represent the directions close to the vertical and horizontal planes, respectively. Obviously, the negative values in Gspine are not the edge information of spine. Then, the Gspine is processed as . where G(n) is the sum of the GFI for the first n column (Fig. 3b), and N is the column number of the image. Since the middle of the spine is nearly straight, the p rows in the middle of the MRI images are selected to detect the spinal edges.

As shown in Fig. 3b, the curve of G(n) is approximately in the horizontal plane in the middle of the spinal region (the middle of the two white lines in Fig. 3a). The process include: first, the centers of the left and right spinal edges (the white crosses in Fig. 3a) are obtained by searching the crossing points for Gspine and center of spine (the white point in Fig. 3a from center to both sides). Second, the search range is limited between the two white lines in Fig. 3a. Third, the left and right spinal edges are obtained by searching the corresponding region from above the centers of left or right spinal edges to both sides, respectively. The Fig. 3c shows the result of spinal edges. Gspine = (2) _∈C , μ∈U1G_,μ − _∈C,μ∈U2 G_,μ Gspine(x, y) = (3)_ Gspine(x, y), Gspine(x, y) ≥ 0 0, Gspine(x, y) < 0 G(n) = (4) _n x=1 (M_+p)/2 y=(M−p)/2 Gspine(x, y), n = 1 . . .N
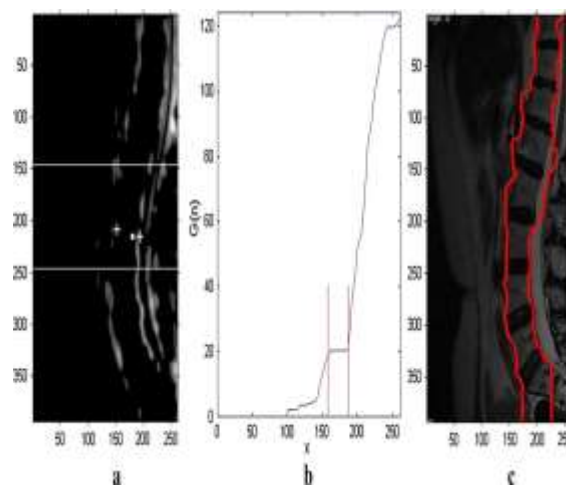

Fig. 3 Detection of spinal curves. **a** Spinal GFI Gspine The white point is the center of the spine, and the *white crosses* are the centers of left and right spinal edges. **b** The sum of the coefficients of the first n columns G(n). **c** The detection of spinal curves.

International Journal of Science Technology Management and Research
Volume 1 , Issue 8 , November 2016
www.ijstmr.com

C.Localization of IVDs

The localization of IVDs is based on GFI information. GFI for localization of IVDs is calculated similar to the process for spines, but the directions of U1 and U2 are different. According to the anatomical knowledge, the angle between the long axis of the IVD and the horizontal line of MRI is almost ± 30°. Therefore, U1 = {7, 8, 9, 10, 11} and U2 = {1, 2, 3, 4, 5} represent directions close to the long axis of IVDs and close to the vertical directions, respectively. The IVDs information image GMdisc (Fig. 4b) is obtained by median filtering (elliptical filter template, long axis: 44 pixels, minor axis: 17 pixels) on the IVDs GFI (Fig. 4a). The searching range of IVDs is narrowed by spinal curves. The process of localization needs some a priori information. The centroid of the IVD is the locating point. In order to obtain the coordinate value of the locating point (XIVD, YIVD), two aspects of a priori anatomical knowledge are adopted:

I)Abscissa x of most IVDs is roughly loca ted in the same vertical line, except for the last few ones that lean slightly to the right;

II) The offsets of vertical y range from 20 mm to 50 mm (25 pixels to 60 pixels in this study). The information of local maximum of GMdisc, combined

a. IVDs GFI

b. IVDs information images GMdisc.

c. Horizontal cumulative curve Gn(n).

d. IVD areas delineation based on localization results

e. IVD edges determined by Gabor feature shown as the superposition of the original image and the binary image.
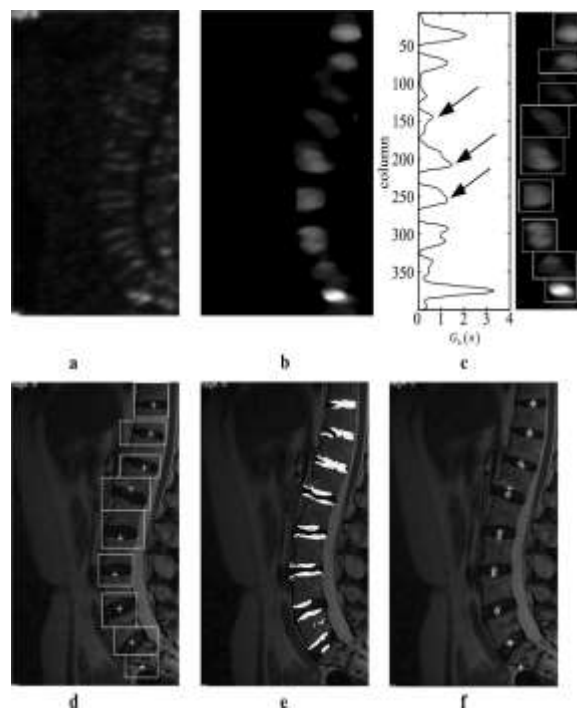
f. Comparison of localization

Fig. 4 IVDs localization information based on the Gabor filter.

(*cross*) and after (*circle*) correction with a priori knowledge, is used for coarse localization. In this process, correction of centre-of-gravity shift is also performed to improve the localization accuracy in case of severe spinal curvature. The process includes:

International Journal of Science Technology Management and Research
Volume 1 , Issue 8 , November 2016
www.ijstmr.com

Step 1: Calculate the horizontal cumulative curve Gh(n) and the candidate vertical coordinate values. Gh(n) is obtained by adding each row with Eq. (5), Where M is the number of rows of the image. The coordinates of local maximum values are the candidates.

Step 2: Calculate the coarse YIVD. According to the a priori information II, the closer points merge into one. The YIVD is achieved after removing the points which do not meet the a priori information II.

Step 3: Calculate the coarse XIVD. The horizontal coordinate XIVD is calculated by a process similar to that for YIVD, but the regions of calculation are different. The mid-values of adjacent two YIVD are taken as boundaries to intercept the IVD part. The same action is performed as Eq. (6) in columns between the two boundaries. The XIVD is obtained based on the a priori information I.

Step 4: Calculate the boxes of IVDs to correct the coarse(XIVD, YIVD). Based on the results of Step 3, the rectangular regions of IVDs (Fig. 4d) are found by the boundary of the local peak of Gh(n) (Fig. 4c) and Gv(n). The upwards and downwards edges of the box in Fig. 4c are calculated by the minimum points and zero points of Gh(n). Then the left and right edges of the box are calculated by the minimum points and zero points of Gv(n) limited by upwards and downwards edges. Figure 4c shows the boxes in GMdisc. Figure 4d shows the boxes in the original image. The angles of IVDs are obtained by analyzing the GFIs information in the rectangular regions.

Step 5: Calculate the accurate center of IVDs (XIVD, YIVD). The binary image of GMdisc is calculated in the boxes obtained in step 3. Figure 4e shows the superposition of the original image and the binary image. Subsequently, the corrected localization of IVDs is obtained by calculating the centroid of the binary image. As shown in Fig. 4f, the white circles are the final localization results (XIVD, YIVD).

D. Segmentation of IVDs

Combining the localization results and spinal curves, the segmentation of IVDs is performed based on GFIs with an adaptive threshold. The main steps include:
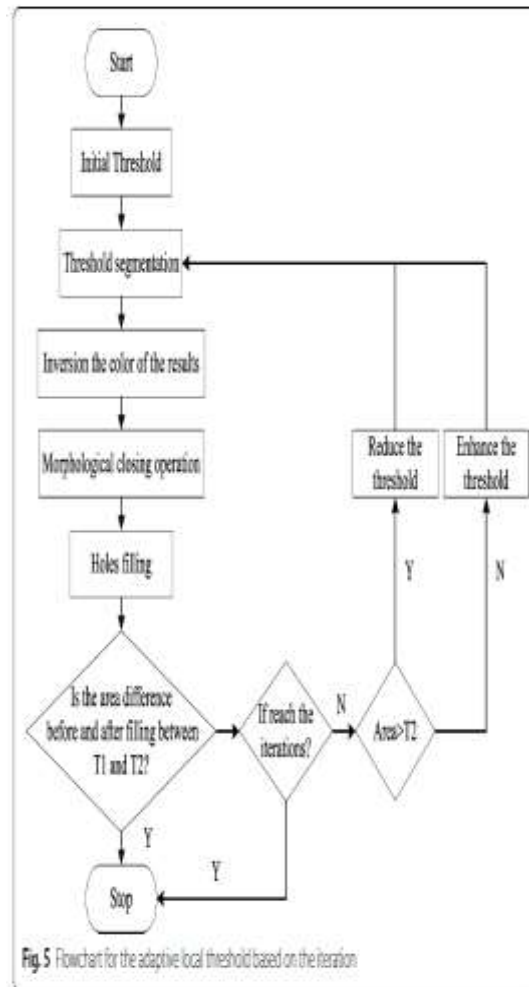
Step 1: Delineate the candidate region of the IVD.

In this region, the average of GFIs of different frequencies $\bar{G}\mu$ is calculated in the direction μ. The maximum $\bar{G}\mu$ can reflect the boundary of the IVD. The $\bar{G}\mu$ in the direction μ with S different frequencies is defined as Eq. (7). The binary image of maximum $\bar{G}\mu$ is obtained using the Otsu method. The up and down boundaries of the candidate region are comprised of the spine curves. The left and right boundaries are comprised of the fitting curve of the outer boundaries of the binary image of maximum $\bar{G}\mu$.

Step 2: Calculate the adaptive local threshold TIVD. Due to the ambiguous boundary and diverse shapes of IVDs, global threshold is not appropriate to segment the IVDs. Therefore, the local threshold (TIVD) of each IVD is adopted to segment the IVDs. As shown in Fig. 5, TIVD is obtained by self-adaption iteration and used for segmentation of IVDs. The initial threshold is calculated by the Otsu method. A1 is the difference between the area of candidate region of the IVD and the area of the binary image of maximum $\bar{G}\mu$. A2 is 1/2 area of the binary image of maximum $\bar{G}\mu$. T1 and T2 are min(A1,A2) and max(A1,A2) area, respectively. The number of iterations is 30.

Step 3: Calculate the coarse segmentation of the IVD. The coarse segmentation results of IVDs are used in steps 2 to 5, in Fig. 5, with an adaptive local threshold TIVD.

Step 4: Post-process for IVD segmentation. The coarse segmentation result may contain holes, non-smooth areas, and superfluous portions. In order to obtain the accurate segmentation, a morphological operator is used: holes filling, erosion, dilation, and five foreground pixels on the background pixel indicate that the pixel is the foreground pixel. When a segmentation result has many connected regions, the largest region is retained.

International Journal of Science Technology Management and Research
Volume 1 , Issue 8 , November 2016
www.ijstmr.com

Fig. 5 Flowchart for the adaptive local threshold based on the iteration

CONCLUSION

The proposed method achieves high accuracy without the need of user interaction, technologist point, or coronal or axial slices. This benefit comes from the shape-recognition ability of the method based on Gabor filter bank. GFIs reduce the localization error by extracting the target information correctly, and correction operation reduces the impact of inaccurate IVD localization by taking all candidate points into account. Due to the interference in direction and morphology in some MRIs, few IVDs were localized outside of the localization results. The results were not significantly affected by the extra localization because recognition techniques, such as areas and morphology, were added.

REFERENCES

1. Ract I, Meadeb JM, Mercy G, Cueff F, Husson JL, Guillin R. A review of the value of MRI signs in low back pain. Diagn Interv Imaging. 2015;96:239–49.

2. Dagenais S, Galloway EK, Roffey DM. A systematic review of diagnostic imaging use for low back pain in the United States. Spine J. 2014;14:1036–48.

3. Lzzo R, Popolizio T, D'Aprile P, Muto M. Spinal pain. Eur J Radiol. 2015;84(5):746–56.

4. Siemund R, Thurnher M, Sundgren PC. How to image patients with spine pain. Eur J Radiol. 2015;84:757–64.

5. Ghosh S, Malgireddy MR, Chaudhary V, Dhillon G. A new approach to automatic disc localization in clinical lumbar MRI: combining machine learning with heuristics. 9th IEEE International Symposium on Biomedical Imaging (ISBI). 2012;114–117.

6. Alomari RS, Corso JJ, Chaudhary V. Labeling of lumbar discs using both pixel-and object-level features with a twolevel probabilistic model. IEEE Trans Med Imaging. 2011;30:1–10.

7. Michopoulou SK, Costaridou L, Panagiotopoulos E, Speller R, Panayiotakis G, Todd-Pokropek A. Atlas-based segmentation of degenerated lumbar intervertebral discs from MR images of the spine. IEEE Trans Biomed Eng. 2009;56:2225–31.

8. Peng ZG, Zhong J, Wee W, Lee JH. Automated vertebra detection and segmentation from the whole spine MR images. 2005 27th Annual International Conference of the IEEE Engineering in Medicine and Biology Society. 2005;2527–2530.

9. Castro-Mateos I, Pozo JM, Lazary A, Frangi AF. 2D segmentation of intervertebral discs and its degree of degeneration from T2-weighted magnetic resonance images. Medical imaging 2014. Comput Aided Diagn. 2014;9035:17.

10. Haq R, Aras R, Besachio DA, Borgie RC, Audette MA. 3D lumbar spine disc segmentation and compression simulation from MRI using shape-aware models. Int J Comput Assist Radiol Surg. 2015;10:45–54.

11. Law MWK, Tay K, Leung A, Garvin GJ, Li S. Intervertebral disc segmentation in MR images using anisotropic oriented flux. Med Image Anal. 2013;17:43–61. Zhu *et al.* BioMed Eng OnLine (*2016) 15:32* Page 15 of 15

12. Chevrefils C, Cheriet F, Grimard G, Aubin C. Watershed segmentation of intervertebral disk and spinal canal from MRI images. Image Anal Recognit. 2007;4633:1017–27.

13. Neubert A, Fripp J, Engstrom C, Schwarz R, Lauer L, Salvado O, et al. Automated detection, 3D segmentation and analysis of high resolution spine MR images using statistical shape models. Phys Med Biol. 2012;57:8357–76.

14. Neubert A, Fripp J, Engstrom C, Walker D, Weber MA, Schwarz R, et al. Three-dimensional morphological and signal intensity features for detection of intervertebral disc degeneration from magnetic resonance images. J Am Med Inform Assoc. 2013;20:1082–90.

15. Oktay AB, Akgul YS. Simultaneous localization of lumbar vertebrae and intervertebral discs with SVM-based MRF. IEEE Trans Biomed Eng. 2013;60:2375–83.

16. Ghosh S, Chaudhary V. Supervised methods for detection and segmentation of tissues in clinical lumbar MRI. Comput Med Imaging Graph. 2014;38:639–49.

18. Kelm BM, Wels M, Zhou SK, Seifert S, Suehling M, Zheng Y, Comaniciu D. Spine detection in CT and MR using iterated marginal space learning. Med Image Anal. 2012;17:1283–92.

19. Daugman JG. Uncertainty relation for resolution in space, spatial frequency, and orientation optimized by twodimensional visual cortical filters. J Opt Soc Am. 1985;2:1160–9.

20. Daugman JG. Complete discrete 2-D Gabor transforms by neural networks for image analysis and compression. Transact Acoust Speech Signal Process. 1988; 36:1169–79.

21. Radman A, Jumari K, Zainal N. Iris segmentation in visible wavelength images using circular gabor filters and optimization. Arab J Foren Eng. 2014;39:3039–49.

22. Hacihaliloglu I, Rasoulian A, Rohling RN, et al. Local phase tensor features for 3-D ultrasound to statistical shape + pose spine model registration. IEEE Trans Med Imaging. 2014;33:2167–79.

23. Shu T, Zhang B. Non-invasive health status detection system using gabor filters based on facial block texture features. J Med Syst. 2015;39:1–8.